Surface segregation and growth-mode transitions during the initial stages of Si growth on Ge(001)2×1 by cyclic gas-source molecular beam epitaxy from Si_2H_6

R. Tsu, H. Z. Xiao, Y.-W. Kim M.-A. Hasan, H. K. Birnbaum, and J. E. Greene
Department of Materials Science, the Coordinated Science Laboratory and the Materials Research Laboratory, University of Illinois, Urbana, Illinois 61801

D.-S. Lin and T.-C. Chiang
Department of Physics and the Materials Research Laboratory, University of Illinois, Urbana, Illinois 61801

(Received 1 July 1993; accepted for publication 13 September 1993)

Surface morphological and compositional evolution during the initial stages of Si growth on Ge(001)2×1 by cyclic gas-source molecular beam epitaxy from Si_2H_6 has been investigated using *in situ* reflection high-energy electron diffraction (RHEED), Auger electron spectroscopy, electron-energy-loss spectroscopy, and scanning tunneling microscopy, combined with post-deposition high-resolution cross-sectional transmission electron microscopy. The layers were deposited using repetitive cycles consisting of saturation Si_2H_6 dosing at room temperature, followed by annealing for 1 min at 550 °C. Film growth was observed to proceed via a mixed Stranski–Krastanov mode. Single-step-height two-dimensional growth was obtained for nominal Si deposition thicknesses t_{Si} up to $\simeq$1.5 monolayers (ML). However, the upper layer remained essentially pure Ge which segregated to the surface through site exchange with deposited Si as H was desorbed. At higher t_{Si}, the Ge coverage decreased slowly, the surface roughened, and two-dimensional multilayer island growth was observed for t_{Si} up to $\simeq$7.5 ML, where bulk reflections in RHEED patterns provided evidence for the evolution of three-dimensional island formula.

I. INTRODUCTION

$Si_{1-x}Ge_x$ alloys and Si/$Si_{1-x}Ge_x$ strained-layer superlattices have attracted increasing attention recently due to their potential for novel electronic and optoelectronic device applications.[1,2] Pseudomorphic strained-layer growth and the degree of interfacial abruptness are often crucial features in these applications. Ge growth on Si(001)2×1 by solid-source molecular beam epitaxy (MBE) proceeds via a Stranski–Krastanov mechanism with a critical layer thickness of 3 monolayers (ML),[3-5] while Si growth on Ge(001)2×1 is thought to occur by three-dimensional island, or Volmer–Weber, growth.[6,7] Hoven *et al.*[8] and Lin *et al.*[9] both observed, using *in situ* core-level photoemission spectroscopy, Ge surface segregation during Si solid-source MBE on Ge(001). Relatively little has been reported, however, concerning the growth mechanism of either Ge on Si or Si on Ge by hydride gas-source MBE (GSMBE),[10,11] where hydrogen may be expected to mediate surface reactions during film growth.

Si_2H_6 has been shown to have advantages as a precursor for low-temperature Si atomic layer epitaxy.[12] Previous studies have demonstrated that Si_2H_6 is dissociatively chemisorbed at room temperature (RT) onto adjacent dangling bonds on Si(001) and further decomposes to SiH_2 and H.[12-15] Site blocking during the adsorption and surface dissociation steps limits the low-temperature surface coverage to $\simeq$0.45 ML.[12] Annealing the Si_2H_6-saturated Si(001) surface at $T_a \gtrsim 350$ °C results in the formation of a monohydride termination that reverts to a clean Si(100)2×1 epitaxial layer by hydrogen desorption at $T_a \gtrsim 550$ °C. Scanning tunneling microscopy (STM) examinations of multilayer Si growth from Si_2H_6 on Si(001) at T_s=550 °C have shown that the surfaces primarily consist of 2×1 terraces bounded by type-A and type-B single-height steps with a few double-layer steps.[15]

The general trends (e.g., Si_2H_6 saturation dose, coverage, and sticking probability) for the adsorption and dissociation of Si_2H_6 on Ge(001)2×1 are similar, but there are important differences associated with the lower energy of the Ge—H bond compared to Si—H and the lower surface energy of Ge than Si.[16,17] For example, hydrogen desorption from Ge monohydride occurs at temperatures that are approximately 150 °C less than those from Si monohydride, and Ge begins to segregate to the surface on Si_2H_6-saturated Ge(001) at an annealing temperature T_a near 350 °C as hydrogen is lost from the Si monohydride phase. Ge segregation proceeds at significant rates at temperatures $\gtrsim$400 °C, and all hydrogen is desorbed through Ge-mediated surface reactions[17] by 450 °C compared to $\simeq$550 °C for Si_2H_6-saturated Si(001).

In this article, we report the results of *in situ* and post-deposition analyses used to follow the surface reaction path of layers deposited on Ge(001)2×1 by repetitive Si_2H_6 dosing and annealing cycles. Cyclic GSMBE was accomplished by exposing the substrate to a saturation Si_2H_6 dose (typically 4×10^{16} cm^{-2}) at RT, followed by annealing at 550 °C for 1 min. Reflection high-energy electron diffraction (RHEED), Auger electron spectroscopy (AES), electron energy-loss spectroscopy (EELS), STM and high-resolution cross-sectional transmission electron

 0021-8979/94/75(1)/240/8/$6.00 © 1994 American Institute of Physics

Downloaded 23 Mar 2004 to 130.126.32.13. Redistribution subject to AIP license or copyright, see http://jap.aip.org/jap/copyright.jsp

microscopy (HRXTEM) were employed to examine surface morphological and compositional evolution. Film growth proceeded via a two-dimensional growth mechanism, in which Ge segregated to the growth surface through site exchange reactions for nominal Si deposition thicknesses t_{Si} up to $\simeq 1.5$ ML. At higher deposition thicknesses, there was a transition to two-dimensional multilayer growth which continued up to $t_{Si} \simeq 7.5$ ML.

II. EXPERIMENTAL PROCEDURE

The growth experiments were carried out in the analytical chamber of a three-chamber stainless-steel 10^{-10} Torr ultrahigh-vacuum (UHV) Si atomic-layer epitaxy (ALE) system.[12,13,16,17] The sample introduction chamber is evacuated with a 330 $l\,s^{-1}$ turbomolecular pump, while the analytical and primary growth chambers are separately pumped to base pressures of $\leqslant 2 \times 10^{-10}$ Torr using both ion and Ti sublimation pumps. During disilane exposure and film growth experiments, the ion and sublimation pumps were valved off, and the analytical chamber was continuously evacuated using the turbomolecular pump.

Disilane flow was regulated via a precision leak valve and introduced into the chamber through a gas doser directed at the Ge surface from a distance of 2.3 cm. The flux incident at the surface was determined by calculating the angular distribution of the effused gas using Clausing's relation.[18] The impingement rate at the sample during disilane exposure was maintained at either $2.1 \pm 0.6 \times 10^{11}$ or $1.0 \pm 0.3 \times 10^{13}$ $cm^{-2}\,s^{-1}$. RHEED, AES, and EELS were available for *in situ* film analyses. The RHEED electron accelerating voltage was set at 20 kV, and the beam was adjusted to intercept the Ge substrates at an angle of approximately 1.5°. First derivative AES spectra were obtained using a primary electron energy $E_p = 3$ keV and a cylindrical mirror analyzer (CMA) with a modulation voltage $V_m = 1.87$ V. EELS spectra were acquired in negative second derivative mode with $E_p = 100$ eV, V_m either 0.50 or 0.63 V, and a primary beam current of less than 0.3 μA.

The Ge(001) substrates used in these experiments were 7 mm$\times$20 mm plates cleaved from 0.4-mm-thick *n*-type wafers (Sb doped, room temperature carrier concentration $= 2.8 \times 10^{14}$–1.5×10^{15} cm^{-3}, resistivity $= 1$–5 Ω cm). Initial cleaning consisted of degreasing by successive rinses in trichloroethane, acetone, methanol, and distilled water. The substrates were then blown dry in dry N_2, exposed to UV irradiation from a low-pressure Hg lamp (15 mW cm^{-2}) for 40 min in air, following the procedure described in Ref. 12, and introduced into the deposition system through the sample-exchange chamber. The wafers were degassed at 250 °C for 1 h and rapidly heated to 450 °C for 5 min to desorb the oxide overlayer. Substrate heating was accomplished resistively by passing current through the sample. Temperature was monitored using both an infrared pyrometer and an alumel-chromel thermocouple attached by a ceramic adhesive to the back of the substrates. Experimental uncertainties in T_s were within ± 20 °C.

Following the *in situ* cleaning procedure, the substrates exhibited sharp 2×1 surface reconstruction patterns typical of clean Ge(001) surfaces, while AES spectra showed no indication of C, O, or other contaminants. During deposition, the substrates were repetitively exposed to Si_2H_6 doses ϕ greater than the saturation dose $\phi_{sat} \simeq 1.1 \times 10^{15}$ cm^{-2} (Ref. 17) at RT and then annealed at $T_a = 550$ °C, after each exposure, for 1 min to desorb the H. The times required to heat the sample from RT to 550 °C and to cool it back down to approximately RT again were $\simeq 10$ s and 1 min, respectively. After each exposure/anneal cycle, the resulting surfaces were analyzed by *in situ* RHEED, AES, EELS, and STM.

STM observations were obtained in a separate UHV system, with a base pressure in the 10^{-11} Torr range (described in detail in Ref. 19). The microscope was operated in constant current mode and all images were obtained with a tunneling current of 0.3–0.35 nA at T_s near room temperature. The same, nominally on-axis, *n*-type Ge(001) wafers described earlier were used as substrates. Sample preparation consisted of degreasing, outgassing in UHV at 500 °C for several hours, and cleaning by repetitive cycles of sputtering with 500 eV Ar^+ ions at a current density of 1–2 μA cm^{-2}, followed by annealing at 800 °C for 15–20 s. This procedure produced clean, ordered 2×1 surfaces, as judged by RHEED, AES, and STM.

Substrate heating in the scanning tunneling microscope was accomplished by passing current through the sample, and temperature was calibrated on an identical test sample using an alumel-chromel thermocouple. Si_2H_6 was introduced into the chamber through a precision leak valve and the dosing pressure, calibrated by an ion gauge and monitored using the ion pump current, was in the range 10^{-8} to 10^{-7} Torr. The pressure readings were corrected using the known ion-gauge sensitivity factor for Si_2H_6, 2.4 relative to air.[20] Following annealing at elevated temperatures, the substrate heating current was switched off and the sample was allowed to cool to near room temperature before STM imaging.

TEM and XTEM analyses were carried out in a Hitachi 9000 microscope operated at 300 kV. Sample preparation for plan-view TEM examination consisted of mechanical grinding followed by Ar^+ ion milling to obtain electron transparent specimens.[21] Specimens for XTEM examinations were prepared by gluing two samples film-to-film and then cutting a vertical section that was thinned by mechanical grinding to a thickness of $\simeq 30$ μm. Final thinning to electron transparency was done by Ar^+ ion milling by which the incident angle and energy were progressively reduced from 20° to 11° and 5 to 3 keV, respectively, in order to minimize radiation damage artifacts and to obtain samples with relatively even thickness distributions.

III. EXPERIMENTAL RESULTS

A. Si_2H_6 adsorption on Ge(001), surface reactions, and hydrogen desorption

Figure 1(a) shows a typical zero-order Laue zone RHEED pattern, taken along the $[\bar{1}10]$ azimuth, from a

Downloaded 23 Mar 2004 to 130.126.32.13. Redistribution subject to AIP license or copyright, see http://jap.aip.org/jap/copyright.jsp

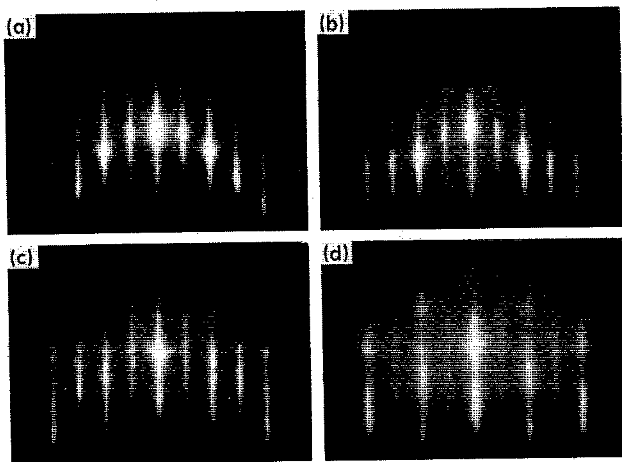

FIG. 1. Typical zero-order Laue-zone RHEED patterns from (a) a clean Ge(001)2×1 surface, (b) after exposure at RT to a saturation Si_2H_6 dose $\phi=1\times10^{16}$ cm^{-2}, (c) after repetitive Si_2H_6-saturation-exposure/annealing (550 °C for 1 min) cycles corresponding to a total Si deposition of $t_{Si}=3$ ML, and (d) as in (c) but with $t_{Si}=7.5$ ML.

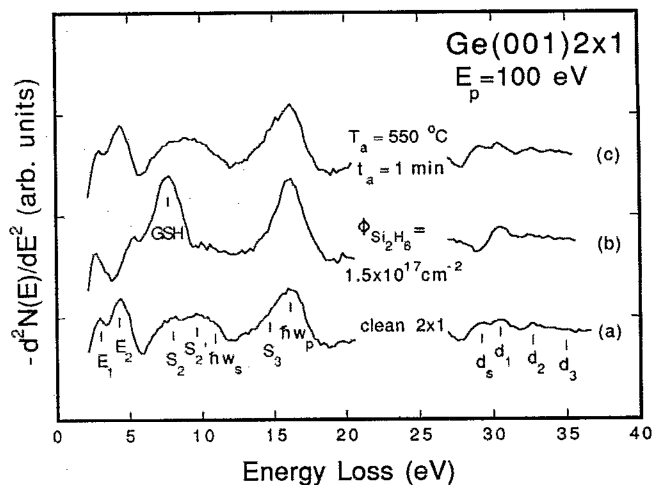

FIG. 3. Typical EELS spectra obtained (a) from a clean Ge(001)2×1 surface, (b) after exposure at RT to a saturation Si_2H_6 dose $\phi=1.5\times10^{17}$ cm^{-2}, and (c) after annealing the Si_2H_6-saturation-exposed sample at 550 °C for 1 min.

clean Ge(001) substrate. The pattern exhibits nearly equal intensities in half-order and fundamental diffraction rods, indicative of a clean well-ordered surface with a (2×1) reconstruction. AES spectra contain only Ge-related features, the dominant ones being the $M_1M_3N_{2,3}$ 47 eV and the $L_3M_{4,5}M_{4,5}$ 1147 eV Ge peaks as shown in Fig. 2(a). No contamination-related peaks, including C and O, were observed.

An EELS spectrum from a clean Ge surface is presented in Fig. 3(a), with peak assignments based upon Ref.

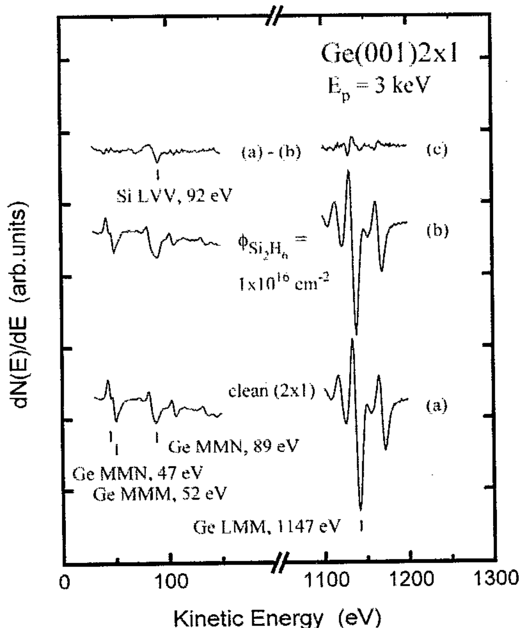

FIG. 2. Typical AES spectra showing the primary Ge peaks obtained from (a) a clean Ge(001)2×1 sample and (b) after exposure at RT to a saturation Si_2H_6 dose $\phi=1\times10^{16}$ cm^{-2}. (c) The difference between two spectra (a) and (b), showing the Si LVV 92 eV peak.

22. E_1 (3.0 ± 0.2 eV) and E_2 (4.4 ± 0.2 eV) are associated with bulk band transitions while $\hbar\omega_s$(10.7 ± 0.2 eV) and $\hbar\omega_p$(16.0 ± 0.2 eV) are due to surface and bulk plasmons, respectively. The features S_2 (7.9 ± 0.8 eV), S_2' (9.3 ± 0.8 eV), and S_3 (14.5 ± 0.8 eV) arise from transitions between backbond states and dangling-bond states in the reconstructed surface. The surface-state transition S_1 at 1.3 eV is lost in the tail of the elastic peak. The higher-energy loss peaks labeled d_s (29.1 ± 0.2 eV), d_1 (30.5 ± 0.2 eV), d_2 (32.9 ± 0.2 eV), and d_3 (34.5 ± 0.2 eV) have been ascribed to transitions between Ge $3d$ core levels ($\simeq29.4$ eV for $3d_{5/2}$ and 30 eV for $3d_{3/2}$)[23] and empty dangling bond (d_s) and conduction band (d_1, d_2, and d_3) states, respectively.[22]

As discussed in detail in Ref. 17, dissociative adsorption of Si_2H_6 on Ge(001) occurs through the reactions

$$Si_2H_6(ad)\rightarrow 2SiH_3(ad)\,, \qquad (1)$$

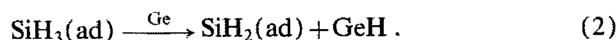

$$SiH_3(ad)\xrightarrow{Ge} SiH_2(ad)+GeH\,. \qquad (2)$$

This results in a reduction in the intensities of the surface dangling bond peaks S_2, S_2', S_3, and d_s as well as a reduction in the surface plasmon peak $\hbar\omega_s$ with respect to $\hbar\omega_p$. The E_1 and E_2 peaks broaden and decrease in intensity as a new feature GSH, a convolution of SiH_2, SiH_3, and GeH peaks, emerges at 8.2 ± 0.2 eV for $\phi\gtrsim1.4\times10^{13}$ cm^{-2}.[17] With increasing exposure, GSH increases in intensity and shifts to lower energy. A typical EELS spectrum from Ge(001) following Si_2H_6 exposure at RT to a saturation dose of 1.5×10^{17} cm^{-2} is presented in Fig. 3(b). The surface dangling bond peaks are no longer observable and GSH is centered at 7.9 eV. Further increases in Si_2H_6 exposure have no measurable effect on the EELS spectra.

Figure 2(b) shows AES results from a Si_2H_6-saturated Ge(001) sample. The intensities of all Ge-related peaks, including the dominant $M_1M_3N_{2,3}$ 47 eV and $L_3M_{4,5}M_{4,5}$ 1147 eV features, were reduced compared to the clean surface spectrum. In addition, new Si-related peaks, such as

Downloaded 23 Mar 2004 to 130.126.32.13. Redistribution subject to AIP license or copyright, see http://jap.aip.org/jap/copyright.jsp

the surface-sensitive $L_{2,3}VV$ transition at 92 eV that overlaps the Ge $M_2M_{4,5}N_{2,3}$ 89 eV peak, emerged. The Si 92 eV peak is better seen by subtracting spectra 2(a) and 2(b) as shown in Fig. 2(c). The Si coverage θ_{Si} was estimated, based upon the ratio of Ge $M_1M_3N_{2,3}$ 47 eV and $L_3M_{4,5}M_{4,5}$1147 eV AES peak intensities I_o before and I_f after each Si_2H_6 exposure, using the following relationship[24]

$$I_f/I_o=(1-\theta_{Si})+\theta_{Si}\exp[-a_{Si}/\lambda_{Ge,Si}\cos\phi)], \qquad (3)$$

where a_{Si} is the [001] thickness of a Si monolayer, $\lambda_{Ge,Si}$ is the inelastic mean free path of Ge Auger electrons—corresponding to the appropriate transition—in Si,[25] and $\phi=0°$ is the Auger electron emission angle with respect to the sample normal. The value of θ_{Si} obtained from Eq. (3), using both the Ge 47 eV and 1147 eV peaks, was approximately 0.5 ML. This is consistent with previous STM results that also showed that the saturate adlayer on Ge is disordered with a few isolated small locally ordered regions.[17] A careful examination of STM micrographs from Si_2H_6 saturation exposed Ge(001) revealed no correlation between Si_2H_6 adsorption and local defects or steps.

A typical zero-order Laue-zone RHEED pattern from a Si_2H_6-saturated Ge(001) surface is shown in Fig. 1(b). The intensities of the half-order reflections are still relatively strong compared to the case for Si_2H_6-saturated Si(001) (in which the saturation coverage is $\simeq 0.45$[12]), where the half-order reflections are essentially unobservable. This is in agreement with previous results showing that a significant fraction of dimerized bonds remain on the Si_2H_6-saturated Ge(001) surface implying that reaction (2) has not gone to completion (i.e., the surface coverage of SiH_2 is <0.5 ML) and that there is still a significant surface concentration of undissociated SiH_3.[17] The 1×1 lattice constant obtained from Fig. 1(b) is 0.556 nm compared to the bulk value, 0.565 nm, obtained from the clean Ge(001) surface.

Annealing Si_2H_6-saturated Ge(001) samples for 1 min at temperatures $T_a\geqslant 150$ °C results in the GSH peak splitting into two components with the main peak located at 7.7 ± 0.2 eV and a shoulder peak at 8.2 ± 0.2 eV. This splitting is quite reproducible. The position of the shoulder peak at 8.2 eV is in good agreement with the reported position for GeH,[26] while the main peak is at a slightly lower energy than our previous results for SiH_2 on Si.[14] These assignments, GeH and SiH_2, are consistent with the peak splitting being caused by the decomposition of residual SiH_3 (i.e., reaction (2) goes to completion). At $T_a=350$ °C, the 8.2 eV shoulder peak disappeared and the S_2' dangling bond peak reemerged indicating H desorption from the Ge surface. With further increases in T_a, Ge surfaces segregation, as indicated, for example, by the appearance and increasing intensities of the E_1, E_2, and d_s peaks, became appreciable and the GSH peak intensity continued to decrease and shift toward the position of SiH at 8.4 eV. Figure 3(c) shows that for $T_a\geqslant 550$ °C, all hydrogen was desorbed and EELS spectra were indistinguishable from the clean Ge surface.

RHEED patterns from Si_2H_6-saturated Ge(001) samples annealed at temperatures $\geqslant 350$ °C exhibited increased half-order, with respect to fundamental, diffraction rod intensities. Over the range $T_a=350$–450 °C, intensity modulations along the diffraction rods were also observed in the zero-order Laue zone, indicating surface roughness. This correlates with the Ge segregation observed in EELS over the same T_a range. The intensity modulations disappeared following 1 min anneals at $T_a>450$ °C as the RHEED patterns and the surface lattice parameter determined from the rod spacings became identical to those obtained from the clean substrate [Fig. 1(a)], consistent with the EELS results.

The Ge $L_3M_{4,5}M_{4,5}$ 1147 eV AES peak intensity was found to increase with annealing temperature for $T_a\gtrsim 350$ °C, while the Si $L_{2,3}VV$ 92 eV peak intensity decreased.[17] AES spectra from samples annealed at $T_a=550$ °C were nearly identical to clean-surface Ge spectra [see, for example, Fig. 2(a)]. The Si $L_{2,3}VV$ peak at 92 eV was barely observable, even in subtracted spectra of the type shown in Fig. 2(c), and the Ge $L_3M_{4,5}M_{4,5}$ 1147 eV peak was approximately equal in intensity to that obtained from a clean Ge(001) surface. These results agree with the EELS and RHEED data already presented and show essentially complete Ge surface segregation.

STM images of a saturation-dosed Ge(001) sample annealed for 1 min at 275 °C showed a much more ordered surface than at room temperature with a higher fraction of the admolecules aligned along one-dimensional chains with lengths of three to six repeat distances. The admolecules, primarily SiH_2 and H (on Ge) from the above results, are thus mobile at this temperature. A STM image of a saturation-dosed sample annealed for 1 min at 330 °C is shown in Fig. 4(a). Complete islanding and considerable island coarsening has occurred with maximum island lengths of $\simeq 12$ nm and aspect ratios of 2–4. Based upon the AES and EELS results described, we believe that these island are primarily composed of SiH. No multilayer islands were observed. Most of the H attached to Ge has been desorbed[16] and well-ordered Ge substrate dimers are visible.

Figure 4(b) shows that increasing T_a to 550 °C resulted in island coarsening and the majority of the anisotropic islands becoming attached to steps leaving relatively few islands, which now have a more rounded and less anisotropic shape, remaining on the terraces. Both effects, island coarsening and step attachment, reduce the step energy term in the total surface free energy. The remaining 2D islands have aspect ratios $\lesssim 3$. The general features observed in Fig. 4(b), irregular step edges and occasional double-height steps, are typical of clean Ge(001)2×1 surfaces whereas Si(001)2×1 exhibits alternating type-A (relatively straight) and type-B (jagged) step edges with essentially no double-height steps at low miscut angles.[15]

B. The early stages of Si growth on Ge(001) by cyclic GSMBE

RHEED patterns, indicative of a well-ordered two-domain 2×1 reconstructed surface, and corresponding

Downloaded 23 Mar 2004 to 130.126.32.13. Redistribution subject to AIP license or copyright, see http://jap.aip.org/jap/copyright.jsp

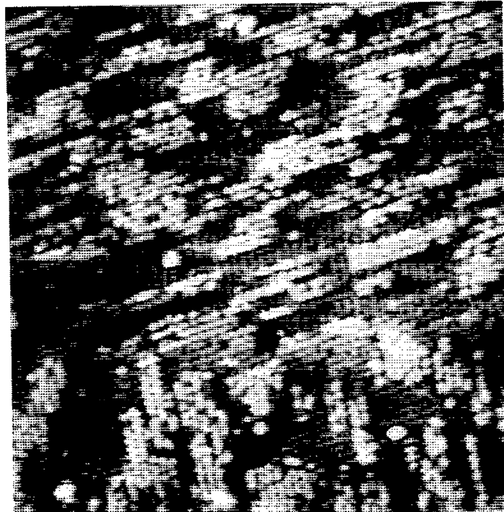
(a)

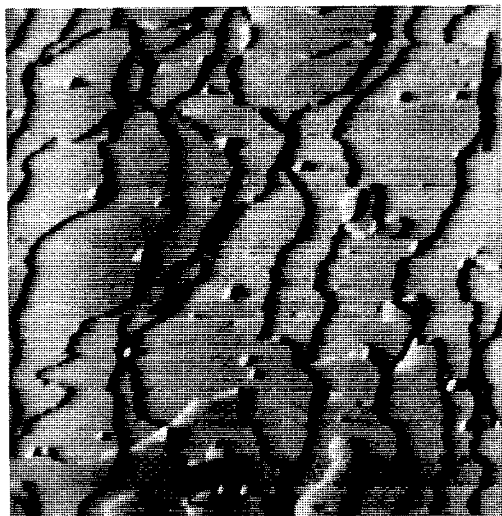
(b)

FIG. 4. (a) A STM image over 500×500 Å^2 area of a Ge(001)2×1 sample that had been exposed at RT to a saturation Si_2H_6 dose $\phi=1.1\times10^{15}$ cm^{-2} and then annealed at 330 °C for 1 min. (b) A 4000 $\times4000$ Å^2 image of a saturation exposed sample annealed at 550 °C for 1 min. The sample bias was −2.0 V.

surface lattice parameters obtained after $t_{Si}\simeq1$ and 1.5 ML deposition/anneal cycles were essentially identical to those from the clean substrate. This is consistent with EELS results. At $t_{Si}\geqslant1.5$ ML, the half-order diffraction rods broadened and decreased in intensity, with respect to fundamental rods, as the background intensity increased. A typical pattern from a sample with $t_{Si}=3$ ML is shown in Fig. 1(c). These results provide evidence of an increasingly rough surface when t_{Si} is increased above 1.5 ML. The gradual formation of the apparent 1×1 pattern indicates a continuous decrease in the average size of 2×1 reconstructed terraces. The full-width at half maximum intensity of a given reflection is proportional to $1/N|\mathbf{a}|$ where N is the number of diffracting units in the surface domain along the direction $\mathbf{a}$. The fundamental diffraction rods also broadened, indicating a corresponding increase in step

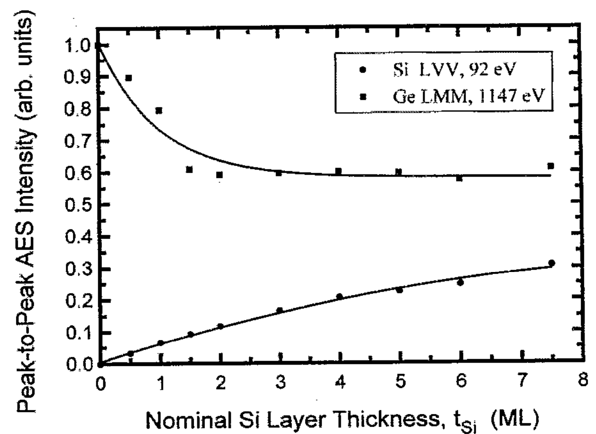

FIG. 5. Peak-to-peak intensities I of the Si LVV 92 eV and Ge LMM 1147 eV AES lines as a function of the nominal Si overlayer thickness t_{Si} deposited on Ge(001).

densities,[27,28] and exhibited intensity modulations along the fundamental rods, implying that the island heights were larger than single atomic dimensions but less than average island widths.

Figure 5 shows the intensities I of Si $L_{2,3}VV$ 92 eV and Ge $L_3M_{4,5}M_{4,5}$ 1147 eV AES peaks as a function of t_{Si}. I_{Ge} decreased with increasing t_{Si} up to $\simeq1.5$ ML and remained approximately constant thereafter, decreasing only very slowly. In contrast, I_{Si} increased continuously over the entire t_{Si} range investigated. The curves in Figs. 5 cannot be fit using standard AES intensity equations,[24] with measured Ge Auger electron escape depths through Si,[25] describing layer-by-layer (Frank–van der Merwe) growth. The curves also did not exhibit typical shapes expected for classical Stranski–Krastanov or three-dimensional island growth.[29] This suggests that Si layer growth on Ge(001) by cyclic GSMBE proceeds via a mixed mode. The slow decay of $I_{Ge}(t_{Si})$, combined with the EELS and RHEED results described and previous reports for Si solid-source MBE on Ge,[30,31] indicates that Ge exchanges sites with deposited Si atoms and segregates to the surface.

STM images of annealed layers with $t_{Si}=$ up to 1.5 ML exhibited single-step-height two-dimensional 2×1 islands that were slightly elongated along dimer row directions and 90° rotated with respect to the underlying terrace. Step densities and surface roughnesses increased with increasing t_{Si} above 1.5 ML as the growth mode changed to 2D multilayer islands, in agreement with RHEED results. Figure 6(a) shows a typical STM image from a layer with $t_{Si}=5$ ML. The 2D islands had an average height of approximately 4 ML with each successive terrace in a given island limited by the finite size of the terrace beneath it. Higher-resolution images such as the one reproduced in Fig. 6(b) showed that the upper layer on the multilayer islands typically exhibited anisotropic shapes composed of single or double dimer rows with an average aspect ratio of $\simeq4$. Some defects such as missing dimers along dimer rows in established islands and antiphase boundaries, due to a displacement of dimer rows by one atom spacing in a ⟨110⟩

Downloaded 23 Mar 2004 to 130.126.32.13. Redistribution subject to AIP license or copyright, see http://jap.aip.org/jap/copyright.jsp

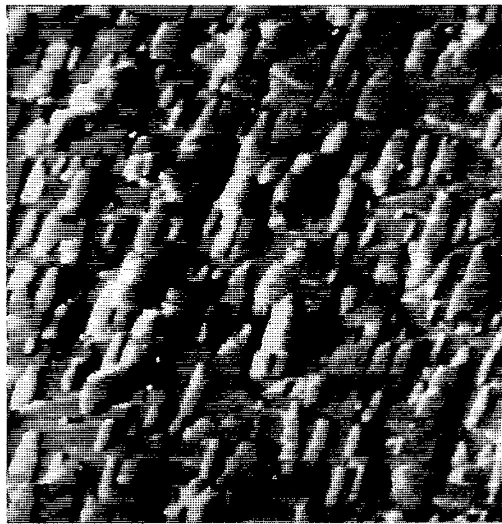

(a)

(b)

FIG. 6. (a) A STM image over a 4000×4000 Å^2 area of a Ge(001)2×1 sample on which a Si overlayer with a nominal thickness of $t_{Si} = 5$ ML had been deposited. (b) A corresponding higher-resolution STM image of (a) obtained over a 500×500 Å^2 area. The sample bias and tunneling current were -2.0 V and 0.3 nA, respectively.

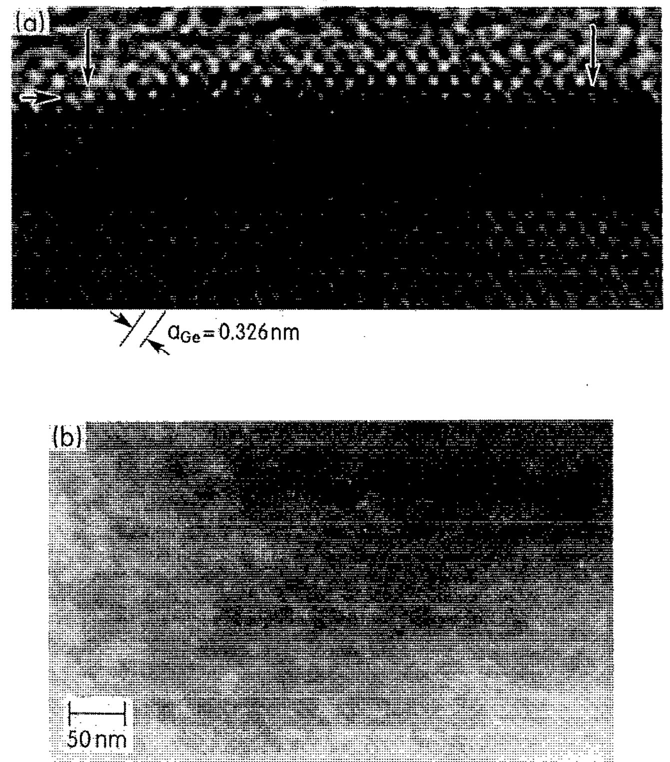

FIG. 7. (a) A high resolution XTEM micrograph showing a typical multilayer island, indicated by arrows, in an overlayer, with a nominal thickness of $t_{Si} = 7.5$ ML, formed on Ge(001) by cyclic Si_2H_6 gas-source MBE. (b) A plan-view TEM micrograph of the sample shown in (a).

direction orthogonal to the dimer rows, were observed [see, for example, Fig. 6(b)]. The high step densities and progressively smaller terraces explain the broadened apparent 1×1 RHEED patterns we observed.

Bulk diffraction spots, indicating the evolution of 2D multilayer growth to 3D island growth, were present in RHEED patterns from layers with $t_{Si} = 7.5$ ML, as shown in Fig. 1(d). Very weak half-order diffraction rods were also still visible.

Figure 7(a) is a typical high-resolution cross-sectional electron micrograph, taken along the [110] zone axis, from a $t_{Si} = 7.5$ ML film, the thickest overlayers grown in the present experiments. No contrast associated with the film/substrate interface was visible and {111} lattice planes were straight and continuous throughout indicating that the overlayer was coherent with the substrate. Several different areas of the sample were imaged in both XTEM and plan-view TEM [see, for example, the 004 bright-field image in Fig. 7(b)], and no dislocations were ever observed. The lack of strain-induced contrast also provided further evidence that the islands were coherent with the substrate. However, the surface of the overlayer contained islands terminated with atomically flat (001) terraces, that STM observations showed to be 2×1 reconstructed, thus explaining the persistence of weak half-order diffraction rods obtained by RHEED. Typical island sizes were 70–100 Å with an average island height of $\simeq 5$ ML.

IV. DISCUSSION

The general criterion for two-dimensional layer-by-layer film growth is

$$\gamma_{f\text{-}v} + \gamma_{s\text{-}f} + \mathscr{E}_f < \gamma_{s\text{-}v}, \tag{4}$$

where $\gamma_{f\text{-}v}$ is the surface energy associated with the formation of the film-vapor interface, $\gamma_{s\text{-}f}$ is the surface energy of the substrate-film interface (which for Ge-Si is expected to be small),[5] $\mathscr{E}_f$ is the elastic energy in the film per unit area of interface, and $\gamma_{s\text{-}v}$ is the gain in surface energy associated with eliminating the initial substrate-vapor interface. In the case of Ge growth on Si, the surface energy of Ge is less than that of Si,[5] and it has been shown both experimentally[3,4] and theoretically[5] that growth by solid-source MBE proceeds in a 2D layer-by-layer fashion for

Downloaded 23 Mar 2004 to 130.126.32.13. Redistribution subject to AIP license or copyright, see http://jap.aip.org/jap/copyright.jsp

three monolayers before the strain energy term, which increases linearly with film thickness due to the lattice constant mismatch ($\simeq 4\%$), becomes large enough that further growth switches to a 3D island mechanism in a Stranski–Krastanov mode.[32] In the case of MBE Si growth on Ge, however, the difference in surface energy acts in the opposite direction and growth is expected to be initiated in the 3D mode, as was observed experimentally.[6,7] In addition, the lower surface energy of Ge acts as a thermodynamic driving force for surface segregation during deposition at elevated temperatures.[33]

In the present experiments involving Si_2H_6 GSMBE on Ge(001), film growth proceeded via a mixed mode. Growth was initiated in a 2D, rather than the expected 3D, mode for t_{Si} deposition up to 1.5 ML. During deposition, hydrogen lowered the surface energy, as opposed to the case of solid-source Si MBE deposition, by eliminating the dangling bonds. In addition, we expect that the presence of surface hydrogen decreases the Si diffusivity, even at elevated temperatures, as was found for the case of Si growth on Si(001) where the aspect ratios of 2D monohydride Si islands obtained from Si_2H_6 GSMBE[15] were shown to be considerably lower than for Si islands obtained by MBE.[34] The initial 0.5 ML of Si on Ge(001) was found by STM to be mostly disordered, with no correlation between adsorbed species and local surface defects or steps.[17] As hydrogen was desorbed during the annealing cycle and the surface energy increased, Ge, which has a lower surface energy than Si, exchanged sites with deposited Si atoms that moved to subsurface regions. RHEED, EELS, and AES observations showed that the $t_{Si}=1$ and 1.5 ML films were terminated with essentially pure Ge surfaces. STM images, which were nearly identical to those obtained from clean Ge(001)2×1 surfaces except for the presence of some single-layer-height islands on terraces, exhibited no evidence of multilayer growth. That is, no more than two levels were exposed on any given terrace.

AES results showed that the Ge coverage decreased slowly with increasing Si deposition thickness $t_{Si} > 1.5$ ML, while RHEED and STM indicated that the surface roughened with the formation of 2D multilayers. This is one of the few reported direct observations of 2D multilayer growth, defined[29] as the condition in which several levels—separated by single-atom-height steps—are exposed on a given terrace while growth proceeds locally in a layer-by-layer mode. RHEED results exhibiting the gradual formation of an apparent 1×1 pattern, indicative of a continuous decrease in the average 2×1 terrace size with increasing t_{Si} above 1.5 ML, are in good agreement with STM observations showing 2D islands in which successive terraces in a given island are smaller and smaller. Since Si adatom mobilities are not expected to be significantly different on Ge than on Si, where cyclic GSMBE from Si_2H_6 occurs in a layer-by-layer mode,[15] we believe that 2D multilayer growth in this case is associated with the pinning of 2D islands at surface defects, such as missing dimers that were observed by STM to be present at significant concentrations around the islands. Such defects, which have been shown theoretically to be due to lattice misfit and anisotropic stress,[35] may also act to inhibit adatom attachment to, and diffusion across step edges.

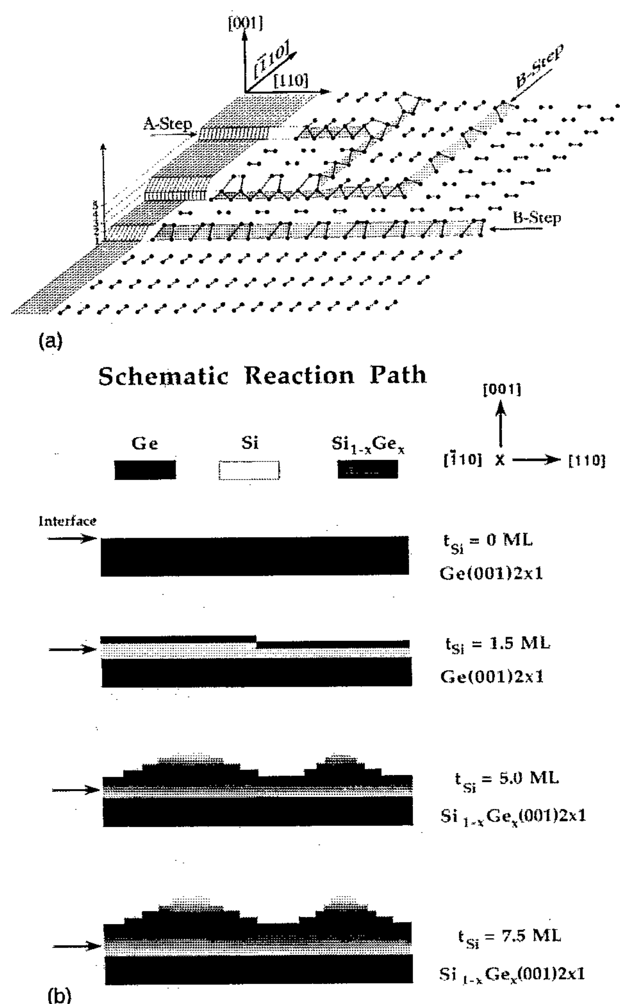

FIG. 8. Schematic diagrams illustrating (a) 2D multilayer island formation with ordered 2×1 dimer rows bounded by type-A and type-B steps and (b) the reaction path as a function of film thickness t_{Si} for overlayer formation on Ge(001) by cyclic Si_2H_6 gas-source MBE.

Due to anisotropies in surface diffusion and bonding on 2×1 reconstructed Si[34] and Ge[36] surfaces (deposited adatoms have higher diffusivities parallel to dimer rows and higher accommodation probabilities at the ends rather than the sides of islands), islands tend to be anisotropic and elongated in the direction perpendicular to the dimer rows in the underlying terrace. 2D multilayer growth is illustrated schematically in Fig. 8(a), where the ragged nature of type-B steps is ignored for simplicity. The length of dimer rows in, for example, terrace 5 (the upper terrace) of Fig. 8(a) is limited by the finite size of the terrace below as the growth of dimer rows along the [110] direction in terrace 5 is halted at type-A steps in layer 4. Similarly, growth on top of the upper terrace, which occurs simultaneously with the filling of terrace 5, will yield even smaller maximum dimer row lengths along [$\bar{1}$10], while the width (maximum number of dimer rows) of the new terrace will be limited by the spatial extent of the overgrown terrace along [110].

Downloaded 23 Mar 2004 to 130.126.32.13. Redistribution subject to AIP license or copyright, see http://jap.aip.org/jap/copyright.jsp

From linear elasticity theory, a fully relaxed Si film on Ge would be expected to have a misfit dislocation number density of the order of 10^{12} cm^{-2} in order to accommodate the $\simeq 4\%$ lattice-constant mismatch. However, HRXTEM, and plan-view TEM results (see, for example, Fig. 7) showed that even the thickest overlayers investigated, $t_{Si}=7.5$ ML, were coherent with the substrate and exhibited no indications of dislocation generation. The formation of a compositionally graded film/substrate interface as well as, for $t_{Si}>7.5$ ML, the development of 2D multilayer islands that are free to elastically contract served to accommodate the strain due to both lattice constant and thermal expansion[37] misfit.

The overall reaction path is summarized schematically in Fig. 8(b). The first 1.5 ML of deposited Si atoms move to the subsurface region due to strong Ge segregation following hydrogen desorption during the 550 °C annealing portion of the growth cycle. EELS, AES, and RHEED results all indicate that the electronic and geometric structure of the surface layer remains essentially identical to that of the initial clean Ge substrate surface. At deposition thicknesses $t_{Si}>1.5$ ML, a 2D multilayer island structure develops and the Ge surface concentration decreases very slowly with increasing overlayer thickness. The overall surface morphology remains approximately the same as the surface "roughness," defined as the average island height, increases from $\simeq 4$ ML at $t_{Si}=5$ ML to 5 ML at $t_{Si}=7.5$ ML, while the average island size decreases.

These results for Si cyclic GSMBE on Ge(001)2×1 give promise for the possibility of Si ALE on Ge, while minimizing or eliminating Ge segregation through hydrogen mediation. From the results of our experiments as well as from theoretical considerations,[38] H passivated Si surfaces have lower surface energies than either bare Si *or* Ge due to termination of the surface dangling bonds. Thus, the driving force for Ge segregation is greatly reduced when the Si overlayer is H terminated. In addition, previous results for UV photostimulated Si ALE on Si(001) from Si_2H_6[12] showed that growth temperatures less than 200 °C were easily achievable. At these temperatures, the segregation rate of Ge during the period between the UV laser pulse giving rise to stimulated hydrogen desorption and the next Si_2H_6 gas pulse will be small due to kinetic limitations.[30,39]

ACKNOWLEDGMENTS

The authors gratefully acknowledge the financial support of the Office of Naval Research through Contract No. N00014-90-J-1241 (J.E.G.) administered by Dr. George Wright, the Semiconductor Research Corporation (J.E.G.) and the US Department of Energy under Grant No. DE-FG02-91ER45439 (H.K.B. and T.C.C.) during the course of this research.

[1] T. P. Pearsall, H. Temkin, J. C. Bean, and S. Luryi, IEEE Electron Device Lett. **EDL-7**, 330 (1986).
[2] T. P. Pearsall and J. C. Bean, IEEE Electron Device Lett. **EDL-7**, 308 (1986).
[3] P. M. J. Maree, K. Nakagawa, F. M. Mulders, J. F. Van Der Veen, and K. L. Kavanagh, Surf. Sci. **191**, 305 (1987).
[4] Y. W. Mo, D. E. Savage, B. S. Swartzentruber, and M. G. Lagally, Phys. Rev. Lett. **65**, 1020 (1990).
[5] J. Tersoff, Phy. Rev. B **43**, 9377 (1991).
[6] H. Kawabata, H. Ueba, and C. Tatsuyama, J. Appl. Phys. **66**, 634 (1989).
[7] M. Copel, M. C. Reuter, E. Kaxiras, and R. M. Tromp, Phys. Rev. Lett. **63**, 632 (1989).
[8] A. J. Hoeven, J. Aarts, and P. K. Larsen, J. Vac. Sci. Technol. A **7**, 5 (1989).
[9] D.-S. Lin, T. Miller, and T.-C. Chiang, Phy. Rev. B **45**, 11415 (1992).
[10] K. Fujinagu, Y. Takahashi, H. Ishii, S. Hirota, and I. Kawashima, J. Vac. Sci. Technol. B **7**, 225 (1989).
[11] P. J. Wang, M. S. Goorsky, B. S. Meyerson, F. K. LeGoues, and M. J. Tejwani, Appl. Phys. Lett. **57**, 814 (1991).
[12] D. Lubben, R. Tsu, T. R. Bramblett, and J. E. Greene, J. Vac. Sci. Technol. A **9**, 223 (1991).
[13] Y. Suda, D. Lubben, T. Motooka, and J. E. Greene, J. Vac. Sci. Technol. B **7**, 1171 (1989).
[14] Y. Suda, D. Lubben, T. Motooka, and J. E. Greene, J. Vac. Sci. Technol. A **8**, 61 (1990).
[15] D.-S. Lin, E. S. Hirschorn, T.-C. Chiang, R. Tsu, D. Lubben, and J. E. Greene, Phys. Rev. B **45**, 3494 (1992).
[16] R. Tsu, D. Lubben, T. R. Bramblett, and J. E. Greene, Thin Solid Films **225**, 191 (1993).
[17] R. Tsu, D. Lubben, T. R. Bramblett, J. E. Greene, D.-S. Lin, and T.-C. Chiang, Surf. Sci. **280**, 265 (1993).
[18] P. Clausing, Z. Phys. **66**, 471 (1930).
[19] F. M. Leibsle, A. Samsavar, and T.-C. Chiang, Phys. Rev. B **38**, 5780 (1988).
[20] R. Imbihl, J. E. Demuth, S. M. Gates, and B. A. Scott, Phys. Rev. B **39**, 5222 (1989).
[21] J.-P. Noel, N. Hirashita, L. C. Markert, Y.-W. Kim, J. E. Greene, J. Knall, W.-X. Ni, M. A. Hasan, and J.-E. Sundgren J. Appl. Phys. **65**, 1189 (1989).
[22] R. Ludeke and A. Koma, Phys. Rev. B **13**, 739 (1976).
[23] T.-C. Chiang, CRC Crit. Rev. Solid State Mater. Sci. **14**, 269 (1988).
[24] M. P. Seah and W. A. Dench, Surf. Sci. **1**, 2 (1979).
[25] P. H. Mahowald, R. S. List, W. E. Spicer, J. Woicik, and P. Pianetta, J. Vac. Sci. Techol. B **3**, 1252 (1985).
[26] L. Surnev and M. Tikhov, Surf. Sci. **138**, 40 (1984).
[27] M. G. Lagally, in *Methods of Experimental Physics*, Vol. 22, edited by R. L. Park and M. G. Lagally (Academic, New York, 1985).
[28] M. Henzler, in *Electron Spectroscopy for Surface Analysis*, edited by H. Ibach, Topics in Current Physics, Vol. 4 (Springer, Berlin, 1977).
[29] C. Argile and G. E. Rhead, Surf. Sci. Rep. **10**, 277 (1989).
[30] F. Fukatsu, K. Fujita, H. Yaguchi, Y. Shiraki, and R. Ito, Appl. Phys. Lett. **59**, 2103 (1991).
[31] F. Fukatsu, K. Fujita, H. Yaguchi, Y. Shiraki, and R. Ito, Surf. Sci. **267**, 79 (1992).
[32] J. E. Greene, in *Multicomponent and Multilayered Thin Films for Advanced Technologies: Techniques, Fundamentals, and Devices*, edited by O. Auciello, NATO Advanced Study Institute (Kluwer, Boston, in press).
[33] P. C. Kelires and J. Tersoff, Phys. Rev. B **63**, 1164 (1989).
[34] Y. W. Mo, B. S. Swartzentruber, R. Kariotis, M. B. Webb, and L. G. Lagally, Phys. Rev. Lett. **63**, 2393 (1989).
[35] J. Tersoff, Phys. Rev. B **45**, 8833 (1992).
[36] G. Xue, H. Z. Xiao, M.-A. Hasen, J. E. Greene, and H. K. Birnbaum, J. Appl. Phys. **74**, 2512 (1993).
[37] *CRC Handbook of Chemistry and Physics*, 71th ed., edited by D. R. Lide, (CRC, Boca Raton, Fl, 1991), pp. 12–54
[38] G. Janssen, J. J. Schermer, W. G. P. Van Enckevort, and L. J. Giling, J. Cryst. Growth **125**, 42 (1992).
[39] T. Tamagawa, T. Shintani, H. Ueba, T. Tatsuyama, K. Nakagawa, and M. Miyao, Thin Solid Films (in press).

Downloaded 23 Mar 2004 to 130.126.32.13. Redistribution subject to AIP license or copyright, see http://jap.aip.org/jap/copyright.jsp